Intensity ratio between Lyman-α_1 and -α_2 lines of hydrogenlike titanium observed in an electron-beam ion trap

Nobuyuki Nakamura,[1] Daiji Kato,[1] Nozomu Miura,[2] Tetsuro Nakahara,[2] and Shunsuke Ohtani[1,2]
[1]*Cold Trapped Ions Project, ICORP, Japan Science and Technology Corp., Chofu, Tokyo 182-0024, Japan*
[2]*The University of Electro-Communications, Chofu, Tokyo 182-8585, Japan*
(Received 16 August 2000; published 4 January 2001)

Lyman-α lines of hydrogenlike Ti^{21+} have been observed with an electron-beam ion trap. The intensity ratio between Lyman-α_1 and -α_2 was measured at electron energies of 10.6, 24.7, and 49.6 keV (2.12, 4.96, and 9.96 in threshold units). The linear polarization of Lyman-α_1 was obtained by comparing the experimental intensity ratio at an observation angle of 90° with the total emission cross section ratio calculated by a simple collisional radiative model. The present results are compared with existing theoretical results.

DOI: 10.1103/PhysRevA.63.024501 PACS number(s): 32.30.Rj, 32.70.Fw, 34.50.Fa, 34.80.Dp

In an electron-beam ion trap (EBIT) [1,2], highly charged ions in the trap region are excited by a monoenergetic, unidirectional electron beam. There have been many investigations using the EBIT for studying fundamental atomic processes in hot plasmas, such as ionization, excitation, and recombination. Because of the low electron density ($n_e \sim 10^{12}$ cm^{-3}), the line intensity observed in the EBIT is generally determined by excitation rates rather than transition probabilities. It is thus useful to measure the line intensity ratio observed at the EBIT for studying electron-impact excitation processes. On the other hand, the angular distributions of the radiation are commonly not isotropic when the excited states are generated by a unidirectional electron beam. The angular distributions and the polarization are determined by the magnetic sublevel distribution of the upper levels, which are important to understand the details of the excitation processes. In addition, polarization measurements are important for plasma diagnostic applications [3]. For example, in solar flares, the presence of magnetic fields creates nonthermal directional electron beams, so that the radiation from such solar flares can be polarized [4].

Polarization measurements with EBITs have been performed for heliumlike Sc [5], heliumlike, lithiumlike, and berylliumlike Fe [6–8], heliumlike and lithiumlike Ti [9], and neonlike Ba [10]. However, the polarization for hydrogenlike ions has never been investigated with the EBIT to our knowledge. In the present study, the intensity ratio between Lyman-α_1 and -α_2 lines of hydrogenlike Ti^{21+} was measured with the Tokyo EBIT [1]. By comparing the observed intensity ratio with the calculated total emission cross section ratio, the polarization of the Lyman-α_1 radiation has been estimated at different interaction energies of the electron beam.

Hydrogenlike Ti^{21+} was produced and trapped in the Tokyo electron-beam ion trap [1,11,12]. The x-ray transitions excited by a 60-μm-diam electron beam were observed with a flat crystal spectrometer [13]. The dispersive plane of the spectrometer was perpendicular to the electron beam. The spectrometer consisted of a flat LiF(200) crystal with an area of 100×50 mm^2 and a position sensitive proportional counter (PSPC) with a cathode of backgammon type [14]. The first order of reflection was used with a Bragg angle θ_B of 39°. The crystal was placed at a distance of 650 mm from the center of the trap and the PSPC was at 350 mm from the crystal. The effective volume of the PSPC was $100\times30\times4$ mm^3 and it was filled with P-10 gas (90% Ar + 10% CH_4) at a pressure of 4 atm. The spectrometer was operated in vacuo ($\sim10^{-7}$ torr) to avoid absorption by air. A beryllium foil with a thickness of 50 μm was used to separate the vacuum of the EBIT ($\sim10^{-9}$ torr) from that of the spectrometer.

Ti was injected with a metal vapor vacuum arc (MEVVA) ion source [15] installed on the top of the EBIT. After injecting ions from the MEVVA, a trap potential was applied to the upper drift tube to produce and trap hydrogenlike Ti^{21+}. The trapped ions were dumped by decreasing the trap potential after the trapping time of 1.5 sec, and then the MEVVA was fired again. This cycle was repeated during the observation. Neon was introduced from a gas injector as coolant. The pressure of neon was 5×10^{-9} torr at the gas injector.

The x-ray intensity in the present measurement is represented as

$$I^{obs} = R_{\parallel} I_{\parallel} + R_{\perp} I_{\perp}, \tag{1}$$

where $R_{\parallel}(R_{\perp})$ and $I_{\parallel}(I_{\perp})$ are the integrated reflectivity and the x-ray intensity, respectively, for the radiation whose electric vectors are parallel (perpendicular) to the electron beam. The intensity ratio between Lyman-α_1 and -α_2 lines is thus represented as

$$\left.\frac{I^{\alpha_1}}{I^{\alpha_2}}\right|^{obs} = \frac{R_{\parallel} I_{\parallel}^{\alpha_1} + R_{\perp} I_{\perp}^{\alpha_1}}{R_{\parallel} I_{\parallel}^{\alpha_2} + R_{\perp} I_{\perp}^{\alpha_2}} = \frac{I_{\parallel}^{\alpha_1}}{I_{\parallel}^{\alpha_2}} \frac{1 + R I_{\perp/\parallel}^{\alpha_1}}{1 + R I_{\perp/\parallel}^{\alpha_2}}, \tag{2}$$

where $R = R_{\perp}/R_{\parallel}$ and $I_{\perp/\parallel} = I_{\perp}/I_{\parallel}$. On the other hand, for electric dipole transitions, the total intensity $\langle I \rangle$ in a 4π solid angle is generally represented by the differential intensity at an observation angle of 90° as

$$\langle I \rangle \propto I_{\parallel}(90°) + 2 I_{\perp}(90°). \tag{3}$$

The intensity ratio for the observation at 90° is obtained from the relation

$$\left.\frac{I^{\alpha_1}}{I^{\alpha_2}}\right|^{obs} = \frac{\langle I^{\alpha_1}\rangle}{\langle I^{\alpha_2}\rangle}\frac{1+2I^{\alpha_2}_{\perp/\parallel}}{1+2I^{\alpha_1}_{\perp/\parallel}}\frac{1+RI^{\alpha_1}_{\perp/\parallel}}{1+RI^{\alpha_2}_{\perp/\parallel}}, \tag{4}$$

or

$$\left.\frac{I^{\alpha_1}}{I^{\alpha_2}}\right|^{obs} = \frac{\langle I^{\alpha_1}\rangle}{\langle I^{\alpha_2}\rangle}\frac{3-P_{\alpha_2}}{3-P_{\alpha_1}}\frac{1+P_{\alpha_1}+R(1-P_{\alpha_1})}{1+P_{\alpha_2}+R(1-P_{\alpha_2})}, \tag{5}$$

where P is the linear polarization defined by

$$P = \frac{I_{\parallel}(90°)-I_{\perp}(90°)}{I_{\parallel}(90°)+I_{\perp}(90°)}. \tag{6}$$

Since the total angular momentum of the upper state is 1/2, the Lyman-α_2 line is unpolarized. Thus, substituting $P_{\alpha_2}=0$ into Eq. (5) yields

$$\left.\frac{I^{\alpha_1}}{I^{\alpha_2}}\right|^{obs} = \frac{\langle I^{\alpha_1}\rangle}{\langle I^{\alpha_2}\rangle}\frac{3}{3-P_{\alpha_1}}\frac{1+P_{\alpha_1}+R(1-P_{\alpha_1})}{1+R}. \tag{7}$$

Consequently, when $\langle I^{\alpha_1}\rangle/\langle I^{\alpha_2}\rangle$ and R are known, the polarization of Lyman-α_1 radiation can be obtained from the present experimental intensity ratio.

We estimated $\langle I^{\alpha_1}\rangle/\langle I^{\alpha_2}\rangle$, i.e., the total emission cross section ratio, using the atomic physics code HULLAC [16]. In the calculations, the radiative cascades from $n=3$ levels were taken into account. Since the present measurement cannot resolve the Lyman-α_2 line from the $2s\rightarrow 1s$ $M1$ transition, the intensity of the $M1$ transition was added to that of the Lyman α_2. The branching ratio for the $M1$ transition from the $2s$ level was estimated from theoretical transition probabilities [17,18] to be 6.9%. For R, we used the theoretical value by Henke *et al.* [19], which is 0.197 at $\theta_B=39°$.

Figure 1 shows x-ray spectra for Lyman-α radiation of hydrogenlike Ti^{21+} obtained at electron energies of (a) 10.6 keV and (b) 49.6 keV. Solid lines represent the Gaussian profiles fitted to the data. In the fitting procedure, the widths of both peaks were assumed to be the same. The intensity ratio between the two peaks was determined from the area of the fitted Gaussian profiles. The experimental intensity ratios obtained are plotted in Fig. 2. Error bars represent the quadrature sum of the statistical errors and the errors arising from the differential nonlinearity of the detector. The differential nonuniformity was measured separately and found to be less than 5% [13], which is less important than the statistical error. As shown in the figure, two independent measurements (''experiment 1'' and ''experiment 2'') were done at $X=2.12$. Between the two experiments, the crystal was turned so that different parts of the crystal and detector plane were used. This was done to examine the effect of nonuniformity in the crystal properties. Although the difference between the two experiments seems rather large, the two measurements agree within the experimental uncertainty. Thus, we summed up the counts in the two experiments. The experimental intensity ratio obtained from the summed data is represented as a solid circle. The crosses in the figure represent the calculated total emission cross section ratios. Assuming that the difference between the total emission cross section ratio and the experimental intensity ratio is due to the angular distribution and the polarization of the Lyman-α_1 radiation, we can obtain the polarization of Lyman α_1 from Eq. (7).

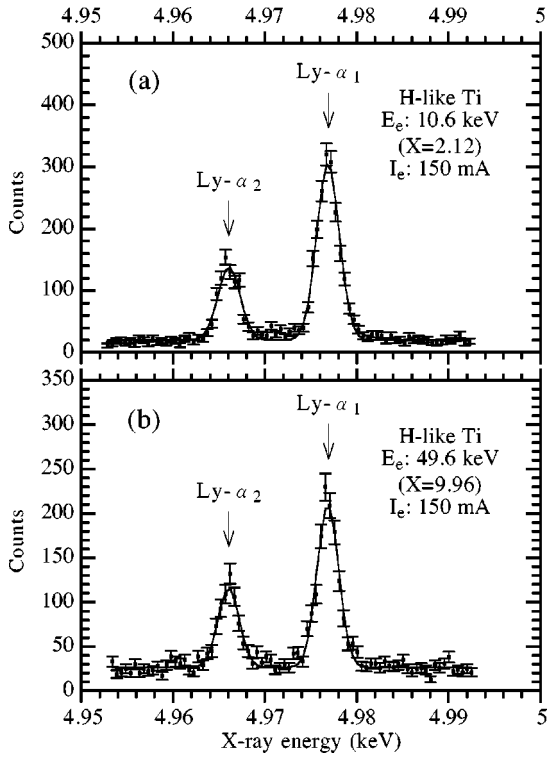

FIG. 1. Spectra of the Lyman-α transitions in hydrogenlike Ti^{21+} taken at electron energies of (a) 10.6 keV and (b) 49.6 keV (X is the electron-beam energy in threshold units). Solid lines represent the Gaussian line shapes fitted to the experimental data. E_e and I_e represent the electron-beam energy and the current, respectively.

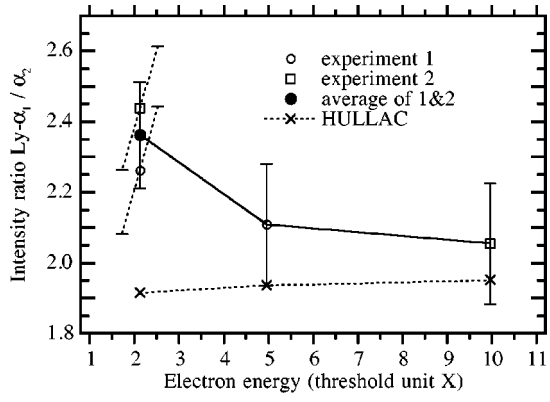

FIG. 2. Experimental intensity ratio between Lyman-α_1 and -α_2 lines as a function of electron energy (threshold unit X). Crosses represent total emission cross section ratio estimated using HULLAC. The values ''experiment 1'' and ''experiment 2'' were obtained in the same experimental condition but the crystal was slightly rotated between them. The error bars for experiment 1 and experiment 2 are drawn as oblique lines to prevent them from overlapping each other.

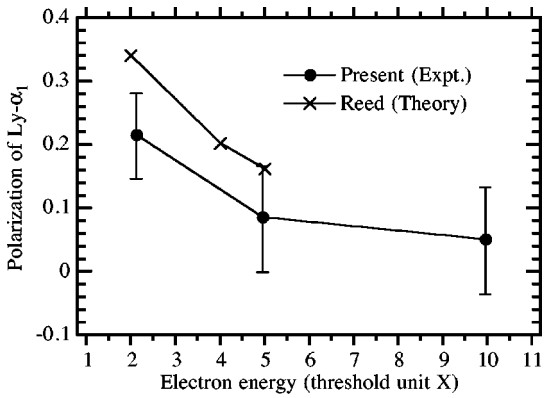

FIG. 3. Polarization of Lyman-α_1 radiation obtained from Eq. (7). Crosses represent the theoretical values [20] calculated by a distorted-wave method. In the theory, only direct excitation was taken into account. (The values in Table II are inconsistent with those in Fig. 3 in Ref. [20]. We ascertained that Table II is correct by private communication with one of the authors, and the values in Table II are used in this plot.

The polarization obtained in this way is shown in Fig. 3. At $X=2.12$, the value obtained from the summed data for experiment 1 and experiment 2 is shown. The theoretical values [20] calculated by a distorted wave method are also plotted in the figure. As seen in the figure, both the experiment and the theory have the tendency that the polarization decreases with increasing electron energy. However, the experimental values are smaller than the theoretical values, especially at $X=2.12$. The following reasons were considered to explain this discrepancy.

(1) Since only direct excitation is considered in the theoretical calculation, indirect excitation such as radiative cascades can give rise to the difference between the experiment and the theory. The contribution from radiative cascades is estimated using HULLAC to be about 5% in the population of the $2p_{3/2}$ level at $X=2.12$. Assuming that the indirect excitation equally populates the $M_J=3/2$ and $M_J=1/2$ sublevels, the polarization of the Lyman-α_1 radiation is revised by only a few percent, which is too small to explain the difference between the theory and the present results.

(2) The electron beam in an EBIT is not truly unidirectional; it has a velocity component $v_\perp$ in the plane that is perpendicular to the magnetic field. This can reduce the polarization. However, the revision is only a few percent even if the electron-beam is inclined by 10° with respect to the magnetic field. Consequently, the influence of $v_\perp$ should be small.

(3) Inside the trap, not only hydrogenlike Ti^{21+} but also bare Ti^{22+} existed. Bare Ti^{22+} can contribute to the population of the $2p$ levels in hydrogenlike Ti^{21+} through a charge transfer (CT) reaction with neutrals (N) in the trap,

$$Ti^{22+}+N\rightarrow Ti^{21+}(nl)+N^+\hookrightarrow Ti^{21+}(2p)+h\nu+N^+, \tag{8}$$

and through radiative recombination (RR) processes,

$$Ti^{22+}+e\rightarrow Ti^{21+}(nl)+h\nu\hookrightarrow Ti^{21+}(2p)+h\nu'+h\nu. \tag{9}$$

These processes could give rise to the difference between the experiment and the theory because only direct excitation is considered in the theoretical calculation. The contribution of RR can be estimated from comparison of the theoretical cross sections for direct excitation and RR. According to the calculations by Moores and Pindzola [21] and by Kim and Pratt [22], the RR cross sections are less than 5% of the direct excitation cross sections at all electron energies studied in the present experiments. Thus the contribution of RR should be small.

The rate of the CT reaction is estimated to be $\sim 0.1\ s^{-1}$, assuming that the neutral density is $10^5\ cm^{-3}$ and the reaction cross section is $10^{-13}\ cm^2$, while the direct excitation rate is estimated to be $\sim 10\ s^{-1}$. Thus the contribution of CT should also be small. However, since the actual value of the neutral density is unknown, the contribution of CT was also examined by measuring the intensity of the Lyman-α line with the electron beam switching on and off. In this measurement, a solid state detector was used to observe Lyman-α transitions. After injecting Ti ions from the MEVVA, the trap potential was applied for 1 s. Subsequently, the electron beam was switched off for 1 ms (the magnetic trapping mode [23]) and switched on again. The x-ray intensity during the magnetic trapping mode was found to be negligibly small compared to that while the electron beam was on. During the time the electron beam was switched off, only CT could contribute to Lyman-α transitions, while both CT and electron-impact excitation could do so while the electron beam was on. Consequently, the contribution of CT to the present polarization measurements should be small. It is noted that after the electron beam was again switched on the x-ray intensity recovered to about one-half of that before the electron beam was switched off; thus at least half the trapped ions existed without escaping from the trap in the magnetic trapping mode.

(4) In Eq. (7), a theoretical value was used for the polarization property R of the crystal. If the actual R value of the present LiF(200) crystal is different from the theoretical value, the experimental polarization should be revised. Since LiF is not a perfect crystal, an individual difference can be large, so that different LiF crystals can have different R values. As an extreme case, if $R=0.54$ (the mosaic limit), the experimental polarization becomes nearly the same as the theoretical value. However, we measured the rocking curve of the present crystal and found that it has a small mosaic spread ($\sim 20''$) which is characteristic for nearly perfect crystals. Thus we believe that the actual R value is not exceptionally different from the theoretical one. Furthermore, we made an observation with Si(111). Si is a perfect crystal, for which the theoretical R value is trustworthy. Although the statistical error was large because of a larger R value (0.621), the polarization obtained from the observation with Si(111) was confirmed to be smaller ($P=0.14^{+0.14}_{-0.16}$) than the theoretical value at $X=2.12$.

(5) For $\langle I^{\alpha_1}\rangle/\langle I^{\alpha_2}\rangle$ in Eq. (7), the theoretical value estimated with HULLAC was used. If this estimation is wrong, the present experimental polarization should be revised. How-

ever, to cancel out the difference between the experiment and the theory, the value $\langle I^{\alpha_1}\rangle/\langle I^{\alpha_2}\rangle$ should be 1.7, which is considered to be improbable.

None of the above contributions can explain the difference between the experiment and the theory. However, since most contributions reduce the polarization, it is possible that a combination of some contributions would make the experimental value close to the theoretical one. Finally, it is noted that 87% of natural Ti elements have no nuclear spin, so that the hyperfine interaction [5] is unlikely to make an important contribution to the polarization.

In summary, we observed the Lyman-α transitions in hydrogenlike Ti^{21+} at electron energies of 10.6, 24.7, and 49.6 keV. From the intensity ratio between Lyman-α_1 and -α_2 lines, the polarization of Lyman-α_1 radiation was experimentally determined. A disagreement was found between the experimental and theoretical polarization especially near the threshold. For further investigation, it will be useful to measure the polarization using two crystals [6] or two spectrometers [10].

A part of this work was done as contract research from the Japan Atomic Energy Research Institute (JAERI). We are grateful to Dr. A. Sasaki of JAERI for fruitful discussions.

[1] N. Nakamura *et al.*, Rev. Sci. Instrum. **69**, 694 (1998).
[2] R.E. Marrs, M.A. Levine, D.A. Knapp, and J.R. Henderson, Phys. Rev. Lett. **60**, 1715 (1988).
[3] T. Fujimoto and S.A. Kazantsev, Plasma Phys. Controlled Fusion **39**, 1267 (1997).
[4] J.M. Laming, Astrophys. J. **357**, 275 (1990).
[5] J.R. Henderson *et al.*, Phys. Rev. Lett. **65**, 705 (1990).
[6] P. Beiersdorfer, J.C. López-Urrutia, V. Decaux, and K. Widmann, Rev. Sci. Instrum. **68**, 1073 (1997).
[7] P. Beiersdorfer *et al.*, Phys. Rev. A **53**, 3974 (1996).
[8] A.S. Shlyaptseva, R.C. Mancini, P. Neill, and P. Beiersdorfer, Rev. Sci. Instrum. **68**, 1095 (1997).
[9] P. Beiersdorfer *et al.*, Phys. Rev. A **60**, 4156 (1999).
[10] E. Takács *et al.*, Phys. Rev. A **54**, 1342 (1996).
[11] F.J. Currell *et al.*, J. Phys. Soc. Jpn. **65**, 3186 (1996).
[12] H. Watanabe *et al.*, J. Phys. Soc. Jpn. **66**, 3795 (1997).
[13] N. Nakamura, Rev. Sci. Instrum. **71**, 4065 (2000).
[14] T. Mizogawa *et al.*, Nucl. Instrum. Methods Phys. Res. A **312**, 547 (1992).
[15] N. Nakamura *et al.*, Rev. Sci. Instrum. **71**, 684 (2000).
[16] A. Bar-Shalom, M. Klapisch, W. H. Goldstein, and J. Oreg, the HULLAC code for atomic physics, 1988 (unpublished).
[17] F.A. Parpia and W.R. Johnson, Phys. Rev. A **26**, 1142 (1982).
[18] V. A. Boiko, V. G. Pal'chikov, I. Y. Skobelev, and A. Y. Faenov, *The Spectroscopic Constants of Atoms and Ions* (CRC, Boca Raton, FL, 1994).
[19] B.L. Henke, E.M. Gullikson, and J.C. Davis, At. Data Nucl. Data Tables **54**, 181 (1993).
[20] K.J. Reed and M.H. Chen, Phys. Rev. A **48**, 3644 (1993).
[21] D.L. Moores and M.S. Pindzola, J. Phys. B **25**, 4581 (1992).
[22] Y.S. Kim and R.H. Pratt, Phys. Rev. A **27**, 2913 (1983).
[23] P. Beiersdorfer, L. Schweikhard, J.C. López-Urrutia, and K. Widmann, Rev. Sci. Instrum. **67**, 3818 (1996).